LETTERS

Photosensitized reduction of nitrogen dioxide on humic acid as a source of nitrous acid

Konrad Stemmler[1], Markus Ammann[1], Chantal Donders[1,3], Jörg Kleffmann[2] & Christian George[4]

Nitrous acid is a significant photochemical precursor of the hydroxyl radical[1–13], the key oxidant in the degradation of most air pollutants in the troposphere. The sources of nitrous acid in the troposphere, however, are still poorly understood. Recent atmospheric measurements[7,10–17] revealed a strongly enhanced formation of nitrous acid during daytime via unknown mechanisms. Here we expose humic acid films to nitrogen dioxide in an irradiated tubular gas flow reactor and find that reduction of nitrogen dioxide on light-activated humic acids is an important source of gaseous nitrous acid. Our findings indicate that soil and other surfaces containing humic acid exhibit an organic surface photochemistry that produces reductive surface species, which react selectively with nitrogen dioxide. The observed rate of nitrous acid formation could explain the recently observed high daytime concentrations of nitrous acid in the boundary layer, the photolysis of which accounts for up to 60 per cent of the integrated hydroxyl radical source strengths[3,6–13]. We suggest that this photo-induced nitrous acid production on humic acid could have a potentially significant impact on the chemistry of the lowermost troposphere.

We first studied this photochemically driven conversion of nitrogen dioxide (NO_2) into nitrous acid (HONO) on films of humic acid (HA), representing the complex unsaturated organic materials ubiquitously present in the environment. We exposed these HA films to various NO_2 mixtures in an irradiated flow-tube and detected the NO_2 and HONO gas phase concentrations at its exit. Typically, 1 mg (8 $\mu g\,cm^{-2}$) of a given HA was coated onto the inner flow-tube wall. Figure 1a shows the results from a typical experiment, where we irradiated such an organic layer in the 400–700-nm wavelength range with an irradiance of 162 $W\,m^{-2}$. A flow of synthetic air containing 20 p.p.b. NO_2 at a relative humidity of 20% passed through the reactor (with a residence time of 0.6 s). During the irradiation we observed a substantial loss of NO_2 and a corresponding formation of HONO of similar magnitude, which was a factor of 30 greater than production in the dark. The high conversion yield of about 80% indicates that NO_2 is reduced by photochemically activated electron donors being present in the organic film and not by a catalysed disproportionation reaction[18]. No comparable reactivity was observed on clean glass surfaces, in contrast to surfaces containing HAs originating from peat, soil or lignite coal (Supplementary Fig. 1). As a consequence, this photochemically driven conversion is probably common to many surfaces 'rich' in partly oxidized aromatic structures, which facilitate the appearance of photochemically activated electron donors. Because such materials are commonly found on ground but potentially also on airborne surfaces[19] (due to soil abrasion, biomass burning or oxidation of volatile organic compounds), the recognition of their photoreactivity may change our understanding of various processes occurring in the planetary boundary layer.

An experiment under the same conditions as that described above was performed over an extended irradiation time of 13 h. Over the total extent of the irradiation 2×10^{15} molecules of NO_2 per cm^2 have been reduced on the HA surface (one molecule per 2,500 daltons of HA). This high value indicates that on average each molecule of HA (average molecular weight ~15 kDa) present in the reactor reacted several times with NO_2. However, the reaction is not catalytic because HA is oxidized by reaction with NO_2. This is consistent with the observation that the reactivity of the HA surface decreased by 55%

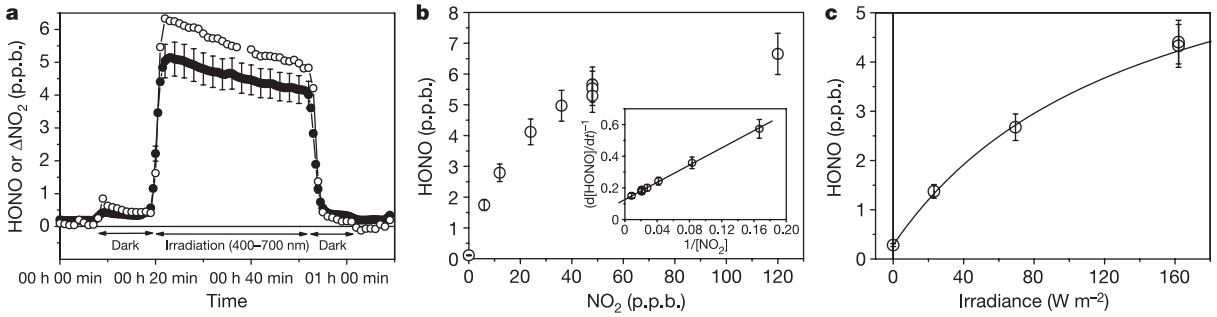

Figure 1 | Conversion of NO_2 → HONO on 1 mg layers of humic acids initiated by visible light (400–700 nm). a, The filled circles represent the concentrations of HONO; the empty circles represent the amount of NO_2 removed during an experiment. **b**, The HONO formation as a function of different initial NO_2 concentrations. In the inset the data of the saturation curve is linearized according to a simple photochemical mechanism (reactions (1)–(3), see Methods section). **c**, The dependence of the HONO formation ($[NO_2]_0 = 20$ p.p.b.) on the light intensity. The black line is a simple model describing the dependence (see Methods section). The error bars ($\pm 2\sigma$) represent the estimated overall accuracy of the chemical analyses.

[1]Paul Scherrer Institut, Laboratory of Radio- and Environmental Chemistry, CH-5232 Villigen, Switzerland. [2]Bergische Universität Wuppertal, Physikalische Chemie/FB C, D-42097 Wuppertal, Germany. [3]Department of Chemistry and Biochemistry, University of Bern, CH-3012 Bern, Switzerland. [4]Laboratoire d'Application de la Chimie à l'Environnement (UCBL-CNRS), F-69622 Villeurbanne, France.

during the 13-h irradiation. HAs are steadily formed by the degradation of biota (about 1 g m^{-2} of soil organic matter is formed per day over the average global continental area[20]), so the deactivation by NO_2 is small compared to the reformation of HA.

Figure 1b shows the effectiveness of the $NO_2 \rightarrow$ HONO conversion at typical tropospheric NO_2 concentrations. The experiments were performed on a single 1 mg HA sample and are corrected for sample deactivation using measured deactivation rates. The HONO yields saturate at high NO_2 concentrations (higher than in the ambient atmosphere) under the reaction conditions described before. An elementary photochemical mechanism—activation of reductive centres (A^{red}) within the organic film by light (reaction (1)), the corresponding deactivation process (reaction (2)), and the reaction of A^{red} with adsorbed NO_2 (reaction (3))—predicts such a saturation (see the Methods section for the mathematical treatment of this reaction system). Compounds 'X' introduced in reactions (1) and (2) indicate that the reactions may involve a photo-induced intra- or intermolecular electron transfer and its back-reaction. Therefore, 'X' should be viewed as oxidants. Clearly, alternative rate-limiting factors, such as a saturation of the adsorption sites by NO_2, might also explain the observed saturation effect.

$$HA \xrightarrow{h\nu} A^{red} + X \quad (1)$$

$$A^{red} + X \rightarrow A' \quad (2)$$

$$A^{red} + NO_2 \rightarrow A'' + HONO \quad (3)$$

The irradiance at the reactor surface in this experiment was about 40% of that corresponding to clear-sky irradiance on a horizontal surface for a solar zenith of 48° in the 300–700-nm range (Supplementary Fig. 2). Thus in the atmosphere the HONO formation can be even more effective.

Figure 1c shows the increase of HONO production with light intensity, which demonstrates the photochemical nature of the reaction. The nonlinearity of the dependency can only be described by reactions (1)–(3), when oxidants 'X' responsible for the deactivation of A^{red} in reaction (2) are photochemically produced transient oxidants (that is, they are formed in reaction (1)). A simple model (see equations (1)–(3) and the Methods section) assuming that the concentrations of oxidants 'X' are proportional to the irradiance is shown in Fig. 1c to match the observations.

The photochemical $NO_2 \rightarrow$ HONO conversion occurs over a broad spectral region with approximate overall quantum yields of about 3.9×10^{-6} (300–420 nm), 1.4×10^{-6} (400–700 nm), and 1.5×10^{-6} (mainly 500–700 nm) at light intensities of 144–162 W m^{-2}, 20 p.p.b. NO_2 and 20% relative humidity (see Supplementary Fig. 2 for lamp spectra). The given values should be taken as a relative measure, because they describe the number of HONO molecules formed per light quantum absorbed by the HA films in the reactor and depend on the experimental parameters (such as thickness of the HA coating or NO_2 concentration). The error in the absolute values is about a factor of two[21]. From the solar spectral distribution, we conclude that the formation of HONO occurs not only in the ultraviolet-A spectral region, where the irradiation can also initiate photodissociation of nitrogen oxides (NO_2, HONO or HNO_3/NO_3^-), but is also very effective in the visible region under atmospheric conditions. This is in contrast to the photolysis of nitrate, which has previously been proposed as a daytime source of HONO[15,22].

In view of the importance of superoxide as an electron carrier in aquatic photochemistry of dissolved organic matter, it is of interest whether superoxide could be the reductant responsible for the $NO_2 \rightarrow$ HONO conversion observed here on solid HA surfaces. Therefore, we performed identical HA irradiations in the absence of NO_2 and measured the yields of H_2O_2, which is the product of superoxide disproportionation ($2O_2^- + 2H^+ \rightarrow H_2O_2 + O_2$). No H_2O_2 was observed under visible light, and only negligible amounts of H_2O_2 in the ultraviolet-A range (0.05 p.p.b., see Supplementary Fig. 3). Additionally, nitric oxide (NO), which exhibits a reactivity[23] towards superoxide in aqueous solution similar to that of NO_2, did not react on the HA surfaces under identical conditions (Fig. 1) when using 20 p.p.b. NO instead of NO_2. The absence of significant amounts of H_2O_2 and the lack of reactivity of NO on irradiated HA surfaces indicate that superoxide is probably not involved in the observed reduction of NO_2.

HAs are a complex mixture of macromolecular organics. They contain aromatic moieties as visible light absorbers and high contents of phenolic functionalities which can act as electron donors and even show (dark) reactivity towards NO_2 (ref. 24). We have previously shown that films of mixtures of synthetic phenols and an aromatic light absorber (a benzophenone) showed a similar $NO_2 \rightarrow$ HONO conversion during ultraviolet-A irradiation, as is observed here for HAs[21]. Such simple mixtures could therefore to some degree be considered as model systems for the photoreactivity of HAs. But we cannot yet assign the exact chemical nature of the reducing intermediates formed on irradiated HAs nor those formed on the synthetic films.

Figure 2a shows the evolution of HONO during irradiation of a

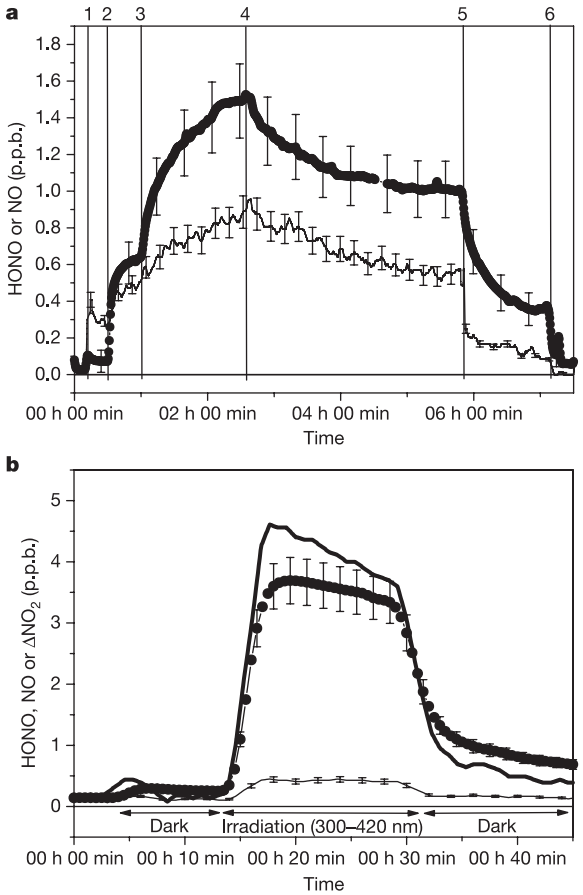

Figure 2 | Conversion of $NO_2 \rightarrow$ HONO on irradiated soil in presence of 17 p.p.b. NO_2 and 30% relative humidity. **a**, The formation of HONO (circles) and NO (line) for an ultraviolet-A irradiation (300–420 nm, 70 W m^{-2}) of 6 g of soil. The vertical lines indicate experimental steps 1 to 6. 1: 00 h 06 min, NO_2 added to air flow; 2: 00 h 30 min, soil exposed to NO_2; 3: 01 h 00 min, irradiation started; 4: 02 h 40 min, irradiation stopped; 5: 05 h 50 min, NO_2 addition stopped; 6: 07 h 07 min, reactor bypassed. **b**, HONO formation (circles) on 20 ± 5 mg artificially acidified soil dust (pH 4.6, H_2SO_4) dispersed on the glass surface of the tubular photo-reactor under ultraviolet-A irradiation (150 W m^{-2}). Thick line, removal of NO_2; thin line, formation of NO. The error bars (±2σ) represent the estimated overall accuracy of the chemical analyses.

natural standard soil (agricultural loamy sand) containing 2.3 wt% organic matter. A 1.5-mm-thick layer of this soil was irradiated (300–420 nm) in a flat-bed flow reactor through a 45 cm × 1 cm glass window by relatively parallel light (70 W m^{-2}). While 45 cm^2 of soil surface were irradiated, a much larger, non-illuminated, internal surface area of at least 5,000 cm^2 (based on the particle sizes) was actually exposed to NO_2. This meant there was already significant HONO production in the dark owing to NO_2 reduction by HAs (by phenolic moieties[24]) or NO_2 disproportionation on humid surfaces[18]. We suggest that the dark reaction observed under our flow-reactor conditions should not be viewed as representative of soil under environmental conditions, where the transport of NO_2 into the bulk soil is probably much more limited. Upon irradiation the HONO formation was markedly enhanced. The slow response of the HONO concentration to switching the light on and off can be related to its high retention on the large soil surface along the reactor. Under these conditions, NO is also observed as a secondary product of HONO at rates consistent with a known dark reaction of HONO with organic soil constituents[25,26]. Figure 2b shows HONO formation on a glass surface containing small amounts of soil dust (0.16 mg cm^{-2}), demonstrating that surfaces contaminated with traces of soil dust (like roads, buildings, rocks or plants) can also be expected to be photoreactive. Owing to the absence of a large bulk volume of soil in the flow tube, the dark reactions of NO_2 and the retention of HONO on the soil surface are drastically reduced in contrast to the photochemical production.

The light-induced HONO production is 2.5×10^{10} molecules cm^{-2} s^{-1} on soil under ultraviolet-A irradiation (70 W m^{-2}) in the presence of 17 p.p.b. NO_2. In the 400–700-nm spectral range we observe HONO photoproduction of 1×10^{10} molecules cm^{-2} s^{-1} for a 75 W m^{-2} irradiance, which is low intensity compared to the solar visible irradiance (for example, 400 W m^{-2} for 48° solar zenith irradiance). From the experimental results, we estimate the total photochemical HONO production to be 5×10^{10} molecules cm^{-2} s^{-1} for a moderately polluted atmosphere (~20 p.p.b. NO_2) and solar irradiances (300–700 nm) of ~400 W m^{-2}. For comparison, Staffelbach *et al.*[16] had to introduce an artificial HONO emission of 3.6×10^{10} molecules cm^{-2}s^{-1} to explain the summer daytime HONO concentrations in southern Switzerland with their model. From their measurements they estimate that HONO contributed by more than 30% to the local radical production in air near the ground during the afternoon[27]. Reports of HONO measurements over a forest[12] and over a rural site[7] inferred unknown daytime HONO sources of 500 p.p.t. h^{-1}and 170 p.p.t. h^{-1}, respectively. From the evaluation of the main radical sources—the photolysis of ozone, formaldehyde and HONO or the ozonolysis of alkenes—the authors concluded that HONO photolysis accounted for 33% of the noon-time radical production[12] and for 24% of the 24-h-average radical production[7]. A photochemical HONO formation at the ground surface of 5×10^{10} molecules cm^{-2} s^{-1} is sufficient to establish these HONO source strengths in air columns (assumed to be homogeneously mixed) with heights of 150 m and 430 m, respectively.

Therefore, we conclude that the photochemical HONO formation described here is consistent with recent observed daytime HONO concentrations and can be predicted to have a large contribution (for example, 20–30%) to the OH-radical production of the lowest hundred to a few hundred metres of the atmosphere. A similar impact can also be estimated by a simple OH-radical budget for the lowermost 100 m of the atmosphere: Summer day primary OH production rates of around 10^7 radicals cm^{-3}s^{-1} are often reported for semi-polluted environments[7,8,12]. Integrating this OH production over a height of 100 m results in a layer production of 10^{11} radicals cm^{-2} s^{-1}. The estimated HONO production of 5×10^{10} molecules cm^{-2}s^{-1} derived in this study could explain half of the observed OH production in this lowermost layer. As the photochemical HONO formation occurs on ground surfaces and HONO photolyses rapidly, this radical source is correspondingly less important for the formation of OH radicals at higher altitudes in the atmosphere. But this lowest part of the atmosphere is important for the oxidation of biogenic volatile organic compounds, which have a similar short atmospheric lifetime[28] as HONO in the daytime atmosphere, and for the formation of secondary air pollutants and aerosols due to the fast radical reactions occurring in this generally most polluted part of the atmosphere.

METHODS

Photoreactors and description of the experiments. The irradiations of HA substrates were performed in 50 cm × 0.8 cm (i.d.) Duran glass tubes installed in an air-cooled lamp-housing holding seven fluorescence lamps (44 cm × 2.6 cm o.d.), in a circular arrangement surrounding the reactor tube. Three types of lamps were used to examine the HONO production under irradiation at different wavelengths (300–420 nm, 400–700 nm and 500–700 nm). The spectral irradiance of the three light sources at the reactor cell surface were measured with a LI-COR 1800 hemispherical, cosine-corrected spectro-radiometer and are shown in Supplementary Fig. 2 and compared to the solar spectral distribution at the Earth's surface and to the absorption spectra of Aldrich-HA. The inner surface of the tubular glass flow reactors (surface = 125 cm^2, surface to volume ratio = 5 cm^{-1}) was coated with a thin layer of HA. The HA coatings on the reactor wall were produced by drying aliquots of aqueous solutions of the HA (1 mg ml^{-1}, pH = 4.4) dispersed on the reactor walls in a nitrogen stream at room temperature. The experiments with soil were performed in a 45 cm × 1 cm × 1 cm Teflon flow reactor with a glass window (45 cm × 1 cm) at the top. This reactor was illuminated by a single fluorescence lamp (70–75 W m^{-2}) mounted in an air-cooled aluminium housing. The flat-bottomed area of the reactor (45 cm^2) was completely covered with soil.

Analytical instrumentation. For the measurement of HONO we used a Long Path Absorption Photometer (LOPAP) instrument[29] (total accuracy ±10%; ref. 29). NO_2 and NO were detected by means of NO/NO_x-chemiluminescence detectors (CLD, Eco Physics, model CLD 77AM, or Eco Physics model CLD AL 770ppt connected to a photolytic converter PLC 760). The total accuracy of the NO_x measurement is estimated to be ±10%. The NO_x detectors were used in combination with a sodium carbonate denuder tube (50 cm × 0.8 cm) at the inlet of the analysers to remove HONO from the gas stream and therefore eliminate the known interference of HONO in the $NO_2 \rightarrow$ NO conversion. H_2O_2 was measured with an Aerolaser AL2001CL gas phase monitor.

Materials and reagents. The HA coatings were prepared from the commercially available HA sodium salts from Aldrich. As a possibly photochemically interfering impurity[30], the specific lot had an iron content of 0.56%. However, spiking of the HA sample solution by additional 1.2% and 3.6% mass portions of iron(III) did not alter the reactivity of the HA coatings significantly. Standard soil was obtained from the Landwirtschaftliche Untersuchungs- und Forschungsanstalt (LUFA), Speyer, Germany. It is a loamy sand (standard soil type Lufa 2.2) collected 15 days before the experiments at 20 cm depth from an agricultural meadow. After drying to 5% residual water content, the soil organic carbon content was 2.29 ± 0.14% and the soil pH was 5.7 ± 0.3.

Model calculations used in Fig. 1. The saturation curve in Fig. 1b can be described according to reactions (1)–(3), assuming a steady-state concentration for $[A^{red}]_{ss}$:

$$\frac{d[HONO]}{dt} = r(HONO) = k_3[A^{red}]_{ss}[NO_2] \quad (4)$$

with

$$[A^{red}]_{ss} = \frac{k_1[HA]}{k_2[X] + k_3[NO_2]} \quad (5)$$

The combination of these two equations results in a HONO formation rate which is first order in NO_2 at low concentrations (that is, $d[HONO]/dt = k_{eff}[NO_2]$), but becomes independent of NO_2 at high NO_2 concentrations (that is, $d[HONO]/dt = k_{max}$). A linear regression (equation (6) of the data in a plot of $r(HONO)^{-1}$ versus $[NO_2]^{-1}$ yields the limiting HONO production $k_{max} = k_1[HA]$ at high NO_2 concentrations from the intercept. k_{max} equals the rate of photochemical production of A^{red}. The first-order rate coefficient $k_{eff} = k_3k_1[HA]/(k_2[X])$ for HONO formation at low NO_2 concentrations is derived from the slope. The linearized plot is presented as an inset in Fig. 1b.

$$r(HONO)^{-1} = \frac{k_2[X]}{k_3k_1[HA]} \frac{1}{[NO_2]} + \frac{1}{k_1[HA]} \quad (6)$$

The available data allow retrieving the maximum HONO production ($k_{max} = (1.1 \pm 0.2) \times 10^{11}$ molecules s^{-1} per cm^2 reactor surface) and the first-order rate coefficient k_{eff} for the HONO formation in the reactor ($k_{eff} = 0.0048 \pm 0.0007$ s^{-1} cm^{-2}; the given value is normalized to 1 cm^2 of

reactor surface area). k_{eff} corresponds to a gas kinetic uptake coefficient of $\gamma = 2 \times 10^{-5}$ for the reaction of NO_2 with the HA surface.

In Fig. 1c the parameters k_{max} and k_{eff} derived above are used to model the dependence of HONO formation on the light intensity. Again we use equation (6), but we assume both that the oxidants [X] in reaction (2) are photochemically produced transient oxidants and approximate the concentration of [X] as proportional to the light intensity and that the rate of formation of A^{red} (reaction (1)) is proportional to the light intensity. The model result is shown in Fig. 1c.

Received 22 July 2005; accepted 16 January 2006.

1. Perner, D. & Platt, U. Detection of nitrous acid in the atmosphere by differential optical-absorption. *Geophys. Res. Lett.* **6,** 917–920 (1979).
2. Platt, U., Perner, D., Harris, G. W., Winer, A. M. & Pitts, J. N. Observations of nitrous-acid in an urban atmosphere by differential optical-absorption. *Nature* **285,** 312–314 (1980).
3. Harrison, R. M., Peak, J. D. & Collins, G. M. Tropospheric cycle of nitrous acid. *J. Geophys. Res.* **101,** 14429–14439 (1996).
4. Harris, G. W. *et al.* Observations of nitrous acid in the Los Angeles atmosphere and implications for predictions of ozone-precursor relationships. *Environ. Sci. Technol.* **16,** 414–419 (1982).
5. Lammel, G. & Cape, J. N. Nitrous acid and nitrite in the atmosphere. *Chem. Soc. Rev.* **25,** 361–369 (1996).
6. Alicke, B., Platt, U. & Stutz, J. Impact of nitrous acid photolysis on the total hydroxyl radical budget during the Limitation of Oxidant Production/Pianura Padana Produzione di Ozono study in Milan. *J. Geophys. Res.* **107,** 8196, doi:10.1029/2000JD000075 (2002).
7. Zhou, X. L. *et al.* Summertime nitrous acid chemistry in the atmospheric boundary layer at a rural site in New York State. *J. Geophys. Res.* **107,** 4590, doi:10.1029/2001JD001539 (2002).
8. Alicke, B. *et al.* OH formation by HONO photolysis during the BERLIOZ experiment. *J. Geophys. Res.* **108,** 8247, doi:10.1029/2001JD000579 (2003).
9. Aumont, B., Chervier, F. & Laval, S. Contribution of HONO sources to the $NO_x/HO_x/O_3$ chemistry in the polluted boundary layer. *Atmos. Environ.* **37,** 487–498 (2003).
10. Vogel, B., Vogel, H., Kleffmann, J. & Kurtenbach, R. Measured and simulated vertical profiles of nitrous acid—Part II. Model simulations and indications for a photolytic source. *Atmos. Environ.* **37,** 2957–2966 (2003).
11. Ren, X. R. *et al.* OH and HO_2 chemistry in the urban atmosphere of New York City. *Atmos. Environ.* **37,** 3639–3651 (2003).
12. Kleffmann, J. *et al.* Daytime formation of nitrous acid: A major source of OH radicals in a forest. *Geophys. Res. Lett.* **32,** 05818, doi:10.1029/2005GL022524 (2005).
13. Acker, K. *et al.* Strong daytime production of OH from HNO_2 at a rural mountain site. *Geophys. Res. Lett.* **33,** 02809, doi:10.1029/2005GL024643 (2006).
14. Kleffmann, J. *et al.* Measured and simulated vertical profiles of nitrous acid—Part I: Field measurements. *Atmos. Environ.* **37,** 2949–2955 (2003).
15. Zhou, X. L. *et al.* Nitric acid photolysis on surfaces in low-NO_x environments: Significant atmospheric implications. *Geophys. Res. Lett.* **30,** 2217, doi:10.1029/2003GL018620 (2003).
16. Staffelbach, T., Neftel, A. & Horowitz, L. W. Photochemical oxidant formation over southern Switzerland. 2. Model results. *J. Geophys. Res.* **102,** 23363–23373 (1997).
17. Honrath, R. E. *et al.* Vertical fluxes of NO_x, HONO, and HNO_3 above the snowpack at Summit, Greenland. *Atmos. Environ.* **36,** 2629–2640 (2002).
18. Finlayson-Pitts, B. J., Wingen, L. M., Sumner, A. L., Syomin, D. & Ramazan, K. A. The heterogeneous hydrolysis of NO_2 in laboratory systems and in outdoor and indoor atmospheres: An integrated mechanism. *Phys. Chem. Chem. Phys.* **5,** 223–242 (2003).
19. Krivacsy, Z. *et al.* Study of humic-like substances in fog and interstitial aerosol by size-exclusion chromatography and capillary electrophoresis. *Atmos. Environ.* **34,** 4273–4281 (2000).
20. Janzen, H. H. Carbon cycling in earth systems - a soil science perspective. *Agric. Ecosyst. Environ.* **104,** 399–417 (2004).
21. George, C., Strekowski, R. S., Kleffmann, J., Stemmler, K. & Ammann, M. Photoenhanced uptake of gaseous NO_2 on solid organic compounds: A photochemical source of HONO? *Faraday Discuss.* **130,** 195–210 (2005).
22. Ramazan, K. A., Syomin, D. & Finlayson-Pitts, B. J. The photochemical production of HONO during the heterogeneous hydrolysis of NO_2. *Phys. Chem. Chem. Phys.* **6,** 3836–3843 (2004).
23. Blough, N. V. in *The Sea surface and global change* (eds Lyss, P. S. & Duce, P. A.) 383–425 (Cambridge University Press, Cambridge, 1997).
24. Ammann, M., Rössler, E., Strekowski, R. & George, C. Uptake of NO_2 on aqueous solutions containing phenoxy type compounds - Implication for HONO formation in the atmosphere. *Phys. Chem. Chem. Phys.* **7,** 2513–2518 (2005).
25. Venterea, R. T. & Rolston, D. E. Mechanisms and kinetics of nitric and nitrous oxide production during nitrification in agricultural soil. *Glob. Change Biol.* **6,** 303–316 (2000).
26. Stevenson, F., Harrison, R. M., Wetselaar, R. & Leeper, R. A. Nitrosation of soil organic matter. 3. Nature of gases produced by reaction of nitrite with lignins, humic substances, and phenolic constituents under neutral and slightly acidic conditions. *Soil Sci. Soc. Am.* **34,** 430–435 (1970).
27. Staffelbach, T. *et al.* Photochemical oxidant formation over southern Switzerland. 1. Results from summer 1994. *J. Geophys. Res.* **102,** 23345–23362 (1997).
28. Atkinson, R. & Arey, J. Gas-phase tropospheric chemistry of biogenic volatile organic compounds: a review. *Atmos. Environ.* **37,** 197–219 (2003).
29. Kleffmann, J., Heland, J., Kurtenbach, R., Lörzer, J. C. & Wiesen, P. A new instrument (LOPAP) for the detection of nitrous acid (HONO). *Environ. Sci. Pollut. Res.* **9,** 48–54 (2002).
30. Zepp, R. G., Faust, B. C. & Hoigne, J. Hydroxyl radical formation in aqueous reactions of iron(II) with hydrogen peroxide—the photo-fenton reaction. *Environ. Sci. Technol.* **26,** 313–319 (1992).

Supplementary Information is linked to the online version of the paper at www.nature.com/nature.

Acknowledgements We thank Y. Abd El Aal, S. Canonica, M. Birrer, J. Dommen, A. Prêvot, L. Urech and I. Alxneit for discussions or technical support. K.S. thanks the Swiss National Science Foundation for support. C.G. acknowledges the grant by Primequal2 for the project SHONO and the CNRS.

Author Information Reprints and permissions information is available at npg.nature.com/reprintsandpermissions. The authors declare no competing financial interests. Correspondence and requests for materials should be addressed to K.S. (konrad.stemmler@psi.ch).